Chapter 10

# Zeolite-Templated Carbon – Its Unique Characteristics and Applications

**Hirotomo Nishihara and Takashi Kyotani**
*Institute for Multidisciplinary Research for Advanced Materials, Tohoku University, Katahira, Sendai, Japan*

**Chapter Outline**



## 10.1. INTRODUCTION

Zeolites have an open structure, which contains regular three-dimensional nanochannels. The shape and the volume of these channels are strictly

**Novel Carbon Adsorbents. DOI: 10.1016/B978-0-08-097744-7.00010-7**

controlled by the framework topology. These channels are the basis of the action of zeolites as molecular-sieve adsorbents or catalysts. In addition, the well-defined nanospace in zeolites can be utilized for synthesizing new materials. The filling of the zeolite nanospace with carbon followed by the extraction of the carbon from the zeolite framework should give rise to the formation of a carbon with a porous structure reflecting the pore structure of the original zeolite template, as shown in the scheme in Fig. 10.1. This is called the "template carbonization method". Base on this idea, about 20 years ago, we started a research to synthesize a unique carbon structure using zeolite Y as a template and polyfurfuryl alcohol as a carbon precursor [1]. Furfuryl alcohol was introduced in the nanochannels of zeolite Y, polymerized and then carbonized. The carbon was liberated from the zeolite network by washing with HF and HCl solutions. The carbon thus obtained exactly reflected the morphology of the zeolite crystalline structure. Some carbon samples had BET surface areas about 1140 $m^2\ g^{-1}$, but, regrettably, it turned out that there was no ordering in pore structure. We therefore examined other combinations of precursors and templates under a wide range of experimental conditions. As a result, in 1997, we obtained carbon with much higher surface area, 2260 $m^2\ g^{-1}$, with a micropore volume as high as 1.1 $cm^3\ g^{-1}$ [2]. However, a substantial volume of mesopores was also present, indicating that the control of porosity was not perfect.

Six years before our publication in 1997 [2], Enzel et al. already made a similar research [3]. They pyrolyzed polyacrylonitrile in the channels of zeolite Y and mordenite, and then liberated the resulting carbons from the zeolites using HF solution to prepare conductive materials by the template method. The carbon obtained had much lower electronic conductivity than the carbon prepared from bulk polyacrylonitrile, suggesting that the spatial limitation in the zeolite channels prevents the formation of the graphitized structure with high conductivity. In 1992, Cordero et al. prepared a carbon/zeolite

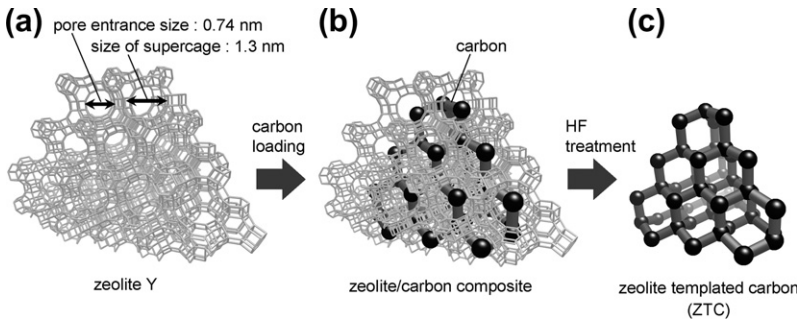


**FIGURE 10.1** Synthesis scheme of the zeolite-templated carbon (ZTC). (a) Zeolite Y template. A Si–O–Si bond is expressed by a line. (b) Carbon/zeolite composite. (c) ZTC liberated from the zeolite template. *(Reprinted with permission from Ref [23]. Copyright 2009 Elsevier)*

composite by the carbon deposition from propylene pyrolysis over zeolite cracking catalyst, followed by the dissolution of the zeolite with HF and HCl solutions to isolate the pyrolytic carbon, and compared the high-temperature oxidation rate of the resulting carbon with other pyrolytic carbons [4]. Six years later, this group reported more detailed characterization results for the resulting carbons [5], which were very similar to those obtained in our study [2]. Johnson et al. reported the carbon preparation using different types of zeolite materials (Y, β, L) [6]. Meyers et al. also used different zeolites (Y, β, ZSM-5) for synthesizing new carbons [7]. These studies showed that all zeolite templates except the L type can endow the resulting carbons with porosity to a greater or lesser extent. However, none of these porous carbons reflected the ordered channel structures of the original zeolite templates. In other words, no one had succeeded in preparing an ordered porous carbon as a negative replica of the zeolite template, until we achieved success in 2000 [8].

The ordered porous carbon we finally prepared is named as zeolite-templated carbon (ZTC). Since the size of the zeolite nanochannels is too small ($<$1.3 nm) to allow the formation of usual carbon stacking structure, ZTC has an extraordinary unique structure, which has never been seen in any carbonaceous materials ever reported. Due to such a unique structure, ZTC is characterized with an extremely large surface area and micropore volume up to 4000 $m^2\ g^{-1}$ and 1.8 $cm^3\ g^{-1}$, respectively, and thereby adsorbs a large amount of molecules or ions. Such properties make ZTC very attractive adsorbents, especially as high-performance energy storage media. In this chapter, we first explain the synthesis method in great detail, where we place special emphasis on how the regular three-dimensional structure of zeolite can be replicated in the resulting carbon structure. Second, we introduce the morphology and structure of ZTC, as well as its unique pore structure. Third, we propose a possible molecular structure of ZTC and emphasize that it is a completely new nanocarbon form. Lastly, we demonstrate the excellent performance of ZTC in the application for hydrogen storage and electric double-layer capacitors.

## 10.2. SYNTHESIS METHOD

To synthesize ZTC, carbon must be uniformly introduced into narrow zeolite nanochannels. The key factors for successful synthesis are: (i) choice of zeolite template and (ii) carbon introduction, which are explained in the following sections.

### 10.2.1. Zeolite

Zeolite is a general name given to a series of crystalline aluminosilicates. Thus far, more than 190 different zeolite crystals have been discovered; however, ZTC can be synthesized only from the specific zeolites having appropriate pore structure, Si/Al ratio, and cation type.

#### 10.2.1.1. Pore Structure

Each type of zeolite has its own pore structure. For ZTC synthesis, the pore entrance size should be as large as possible, from the following two reasons:

1. To avoid pore blocking during carbon introduction.
2. To form robust carbon framework which can retain the ordered network structure after the template removal.

The pore entrance of zeolite is usually a ring of O–Si–O chain, and the pore entrance size depends on the number of O atoms included in the ring. For example, the pore entrances of zeolite A and MFI are oxygen 8- and 10-membered rings, respectively, and they are too small to allow enough carbon introduction inside the zeolite micropores [9]. On the other hand, zeolites with 12-membered ring, such as zeolite Y (X), zeolite β, zeolite L, and mordenite, enable enough carbon filling [9].

Not only pore entrance size but also pore connection topology is significantly important. To obtain porous carbon replica with ordered framework like the structure shown in Fig. 10.1c, zeolite should have three-dimensionally connected micropores. Thus far, only zeolite Y (X) [8–10], zeolite β [9,11], and EMT [12] have been successfully used as hard templates for obtaining porous ZTC with high structure regularity. On the other hand, zeolites with one-dimensional micropores, such as zeolite L and mordenite, give one-dimensional carbon frameworks which do not retain structure regularity of the zeolite templates [9].

#### 10.2.1.2. Si/Al Ratio

Zeolites usually have strong acidity, which plays a significant role for the uniform carbon deposition by chemical vapor deposition (CVD). This is one of the key processes to obtain ZTC with high surface area (see Section 10.2.2 for details). It is well known that the acid sites in zeolites catalyze the formation of polycyclic aromatic compounds called "coke". In the CVD process, due to the catalysis, it is possible to convert the hydrocarbon gas below its decomposition temperature into a carbonaceous structure inside the zeolite micropores, and a significant deposition of pyrolyzed carbon outside the zeolite particles can be avoided. Zeolites with poor acidity such as silicalite-1 therefore cannot be used as hard templates.

The origin of the strong acidity is Al-substituted sites in the zeolite framework. Accordingly, smaller Si/Al ratio gives larger acid site amount. The preferable Si/Al ratio for ZTC synthesis is below 20. It should be noted that zeolites containing too large amount of Al generally have poor heat stability. For example, zeolite A (Si/Al = 1) and zeolite X (Si/Al < 2) lose their crystal structures around 900 °C even if they contain carbon inside their micropores.

#### 10.2.1.3. Cation Type

Each Al site in the zeolite framework has an exchangeable cation, and the cation type dominates the strength of the acid catalysis. Proton ($H^+$) gives

a very strong acidity, thereby enhancing carbon deposition. In this case, zeolite micropores are easily blocked and carbon is deposited not only inside zeolite micropores but also outside. Transition metal ions, such as $Ni^{2+}$ or $Co^{2+}$, give further high catalytic activity, and in some cases, even carbon nanotubes are generated [13,14]. The moderate catalytic activity is provided by $Na^{+}$ cation, producing ZTC with high structure regularity as well as high surface area [8].

## 10.2.2. Carbon Introduction

There are three methods for the carbon introduction into the zeolite micropores.

1. Polymer carbonization which consists of the introduction of organic monomers, followed by polymerization and carbonization [2,6,15–18].
2. CVD method using small organic molecules as carbon sources [2,5,11,19,20].
3. Tow-step method which consists of the polymer carbonization followed by further CVD [8,21].

### *10.2.2.1. Polymer Carbonization*

In the polymer carbonization, organic monomers are first introduced inside the nanochannels of zeolite and then they are polymerized. If the polymerization is proceeded by acid catalyst like the case of poly(furfuryl alcohol), zeolite itself can catalyze the polymerization. If this is not the case like poly(acrylonitrile), γ-ray radiation can be used for the polymerization in the zeolite [2]. This method allows uniform carbon introduction and is useful especially for zeolites with large particle sizes [16]. However, a large fraction of the organic polymer formed inside zeolite micropores is generally decomposed during carbonization step, and the resulting carbon framework tends not to be robust enough to retain high structure regularity after the removal of the zeolite template. Therefore, it is difficult to obtain ZTC with very high surface area by the polymer carbonization.

### *10.2.2.2. CVD Method*

CVD method allows stuffing larger amount of carbon into zeolite micropores than the case of the polymer carbonization, and therefore the resulting carbon framework can be strong enough. In this method, a carbon source, e.g. hydrocarbon gas, is attached to zeolite below the decomposition temperature of the carbon source gas itself, and the zeolite catalyzes carbon deposition. Considering such a mechanism, the carbon source molecules should be as small as possible so that the source molecules can pass through the zeolite micropores even after narrowing by carbon deposition. Figure 10.2 illustrates the pore entrance (oxygen 12-membered ring) of zeolite Y before (Fig. 10.2a) and after (Fig. 10.2b) carbon deposition, together with several hydrocarbons

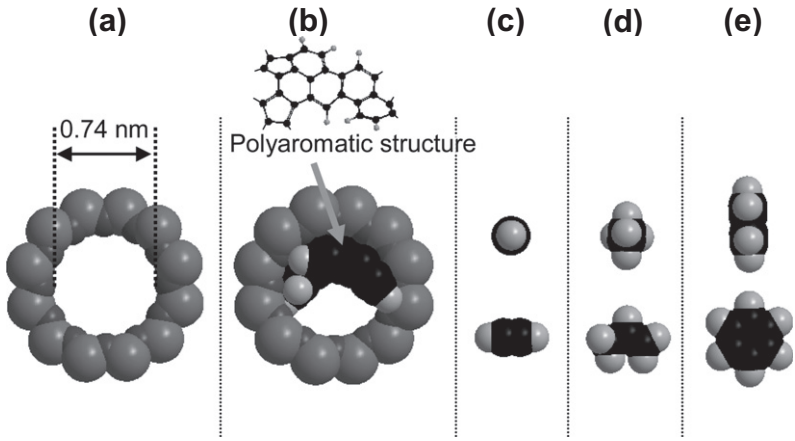


**FIGURE 10.2** The pore entrance structure of zeolite Y (a) before and (b) after carbon deposition, and molecular images of (c) acetylene, (d) propylene, and (e) benzene (views from different angles). Polyaromatic structure shown in (b) is a fragment of the molecular model of ZTC shown later (Fig. 10.11c).

(Fig. 10.2c–e). Note that polyaromatic structure shown in Figure 10.2b is a fragment of the molecular model of ZTC shown later (Fig. 10.11c), i.e. this is a part of Fig. 10.11c. Acetylene (Fig. 10.2c) and propylene (Fig. 10.2d) can pass through the narrowed micropore (Fig. 10.2b), whereas it seems to be difficult for benzene (Fig. 10.2e). Acetylene is the smallest hydrocarbon and very well suitable as a CVD source for producing high-quality ZTC easily [19]. Not only hydrocarbons but also nitrogen-containing compounds, such as acetonitrile, can be used as a CVD source, and in this case, nitrogen-doped ZTC is obtained [11,22].

The operating conditions of CVD, such as temperature, period, and concentration of the CVD source gas, significantly affect the quality of the resulting ZTC.

As for the CVD temperature, higher temperature generally enhances carbon deposition. However, if the CVD temperature is too high, the CVD source molecule is decomposed not only in zeolite nanochannels but also in a vapor phase, and a large amount of carbon is deposited also outside zeolite particles. The self-decomposition temperature of acetylene and propylene are about 650 and 750 °C, respectively. In order to avoid carbon deposition outside the zeolite particles, the CVD temperature should be lower than the self-decomposition temperature.

The longer CVD time also increases the amount of carbon deposition. Below the self-decomposition temperatures, however, carbon deposition can be saturated after a certain period. For example, in the case of acetylene CVD on NaY zeolite at 600 °C, carbon deposition amount at first increases with

increasing the CVD time, and the amount reaches ca. 28 wt% after 4 h. This is the maximum and no further carbon is deposited anymore.

The concentration of the CVD source gas is also a key factor for the carbon deposition. Under a fixed CVD temperature and time, larger concentration enhances carbon deposition.

Since the carbon deposited by CVD does not yet have a robust network structure at this moment, if zeolite is removed soon after the CVD, the ordered structure is likely to be lost. To stabilize the carbon framework, a high-temperature treatment is essential. The temperature of this treatment should be as high as possible. The upper limit of the temperature depends on the heat stability of zeolite: most of zeolites are not stable above 1000 °C.

#### *10.2.2.3. Two-step Method*

The two-step method takes over the advantages of each of two methods, i.e. uniform carbon deposition by the polymer carbonization and robust carbon framework by the CVD method. It is therefore possible to obtain ZTC with high structure regularity having very high surface area. Our group have actually demonstrated the synthesis of ZTC with an extremely high surface area of 4100 $m^2 g^{-1}$ [21].

## 10.3. STRUCTURE OF ZTC

ZTC has a very unique structure which is completely different from conventional porous carbons, such as activated carbons, and this gives rise to its extraordinary adsorption properties. In this chapter, its basic structure found by electron microscopy, X-ray diffraction (XRD), and $N_2$ physisorption is explained.

### 10.3.1. Bulk Shape

ZTC is obtained as a negative replica of zeolite template. As a result, the bulk shape of the zeolite template is also replicated by ZTC. Figure 10.3 shows scanning microscopy (SEM) images of two zeolites with different particle sizes (Fig. 10.3a: 200 nm, Fig. 10.3b: 2 μm) and the resulting ZTCs from them (Fig. 10.3c and d). It is clearly seen that the bulk shapes of the zeolite templates are well transferred to the corresponding ZTCs. Thus, the bulk shape of ZTC can be controlled by changing the morphology of the zeolite template.

### 10.3.2. Ordered Structure

Figure 10.4 shows transmission electron microscopy (TEM) images of ZTC synthesized from zeolite Y. A low magnification image (Fig. 10.4a) shows that the shape of ZTC is polygonal particles which are derived from zeolite template, as was found from Fig. 10.3a. Besides bulk shape, microscopic

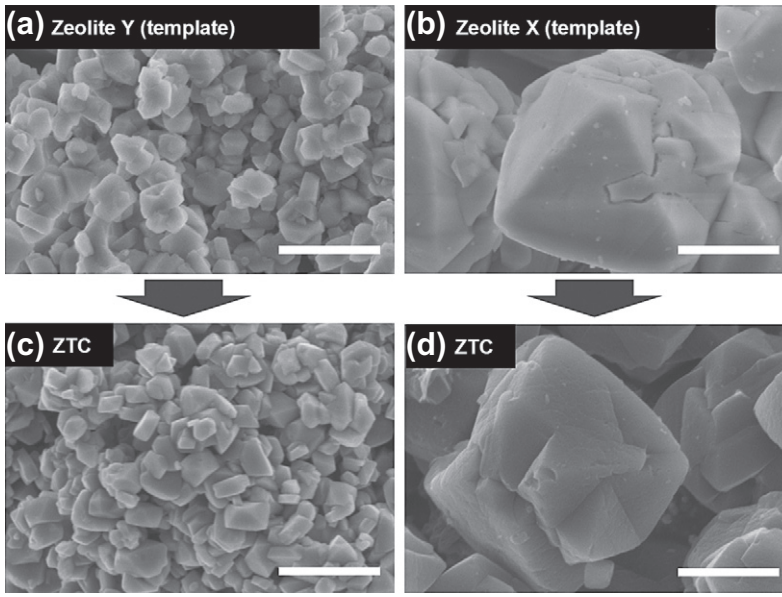


**FIGURE 10.3** SEM images of (a) zeolite Y (particle size is ca. 200 nm), (b) zeolite X (particle size is ca. 2 μm), (c) ZTC from zeolite Y and (d) ZTC from zeolite X. Scale bar is 1 μm.

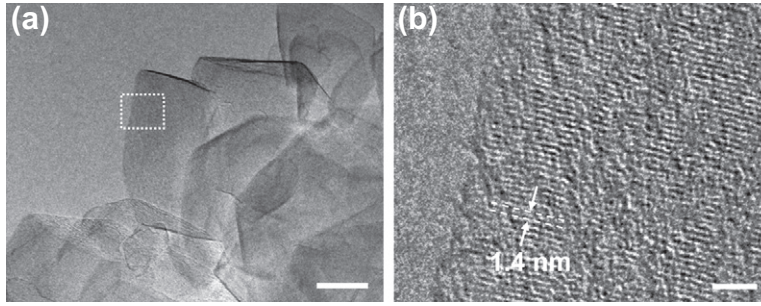


**FIGURE 10.4** TEM images of ZTC obtained from zeolite Y. (b) shows an enlarged image of a part surrounded with a white square in (a). Scale bars in (a) and (b) are 100 and 10 nm, respectively.

structure of zeolite template is replicated by ZTC. A high magnification image (Fig. 10.4b) clearly shows zeolite-like fringes with a periodicity of 1.4 nm, corresponding to zeolite (111) plane.

Figure 10.5 shows XRD patterns of zeolite Y and the resulting ZTC. Generally, disordered carbons show broad peaks around $2\theta = 26°$ and 44° corresponding to carbon (002) and (10) peaks, respectively. However, ZTC with high structure regularity usually does not show these peaks, indicating that

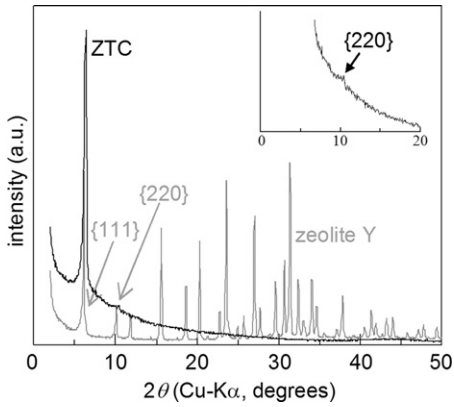


**FIGURE 10.5** XRD patterns of zeolite Y and ZTC obtained as a replica. *(Reprinted with permission from Ref [23]. Copyright 2009 Elsevier)*

this carbon contains neither graphene-stacking structure nor large and flat graphene plane. Instead, ZTC has a sharp peak around $2\theta = 6.4°$ and also has a weak peak at $2\theta = 10.4°$. These peaks correspond to (111) and (220) planes derived from the zeolite template [23]. If the synthesis of ZTC is not successful, its XRD pattern shows broad peaks of carbon (002) and (10). There are two possible reasons for the appearance of these peaks. One possibility is the formation of disordered carbon shell outside zeolite micropores as shown in Fig. 10.6. In this case, the surface area of ZTC becomes lower, because such outside carbon is usually nonporous. The other possibility is a collapse of carbon framework. If carbon introduction into zeolite micropores is not enough, or if heat treatment for structure stabilization is not enough, carbon framework is partly destroyed upon the zeolite removal and graphene sheets formed inside the zeolite nanochannels are aggregated and/or stacked. Also in this case, the surface area of ZTC decreases significantly.

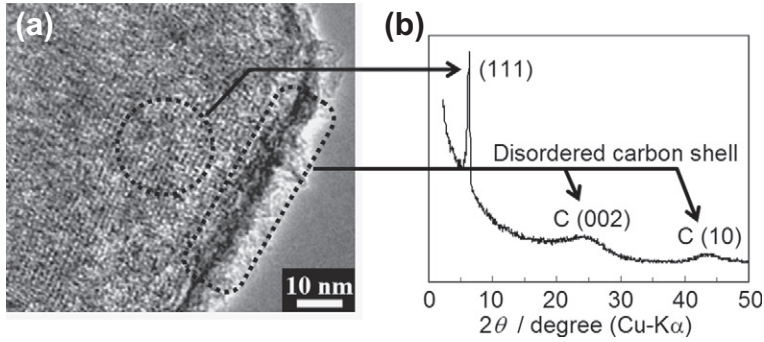


**FIGURE 10.6** (a) A TEM image and (b) XRD patterns of ZTC containing a disordered carbon shell formed outside zeolite micropores.

## 10.3.3. Textural Properties

### *10.3.3.1. Analysis by $N_2$ Physisorption*

Figure 10.7a shows $N_2$ isotherms of ZTC synthesized from zeolite Y and commercial activated carbons: MSC30 (Kansai Coke and Chemicals Co., Ltd.) and A20 (Unitika, Ltd.). ZTC has a typical type I isotherm by IUPAC definition, indicating that it is a microporous carbon. On the other hand, the isotherms of A20 and MSC30 are slightly deviated from the typical type I isotherm, with regard to adsorption increase around $p/p_0 = 0.1 \sim 0.3$, especially in MSC30. The adsorption in this pressure range corresponds to the presence of small mesoporous with the size of 2–4 nm [24–26]. Figure 10.7b shows pore-size distributions calculated by the density functional theory (DFT) method. As was indicated from their isotherms, MSC30 and A20 have broad distributions in the range of 1–3.5 nm. On the other hand, ZTC shows a sharp peak at 1.2 nm.

The BET surface areas and pore volumes calculated from the $N_2$ isotherms are summarized in Table 10.1. MSC30 is a highly activated carbon produced by KOH chemical activation, and has a very high BET surface area of 2690 $m^2\ g^{-1}$, which is almost the upper limit for conventional activated carbons. However, ZTC has a further higher BET surface area of 4030 $m^2\ g^{-1}$. Another remarkable feature of ZTC is its very large micropore volume (1.69 $cm^3\ g^{-1}$) without mesopores. In the case of a conventional activation method, not only micropores but also mesopores are inevitably formed, especially by deep activation for obtaining high surface area. MSC30 thus has a large total pore volume of 1.73 $cm^3\ g^{-1}$, but the fraction of micropores is no more than 65% due to the presence of significant mesopores. In the case of ZTC, 95% of its total pore volume is of micropore volume (Table 10.1). Having very high surface area without the presence of mesopores is important especially for energy-storage applications such as hydrogen storage and electric

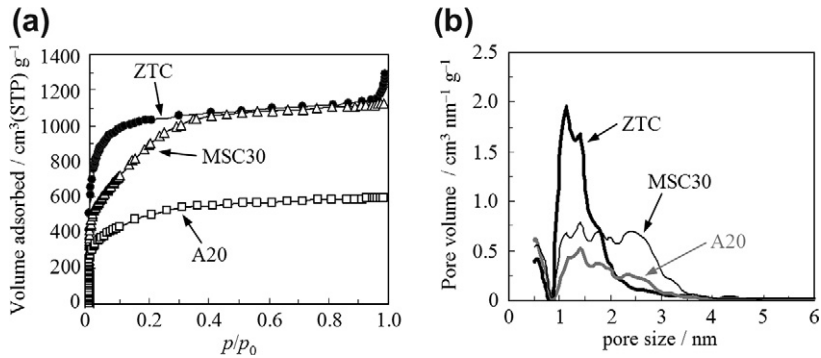


**FIGURE 10.7** (a) $N_2$ adsorption–desorption isotherms and (b) pore-size distributions of ZTC synthesized from zeolite Y and commercially activated carbons (MSC30 and A20).

**TABLE 10.1** BET Surface Areas and Pore Volumes of ZTC and Activated Carbons

| Sample | $S_{BET}$[a] $m^2\ g^{-1}$ | $V_{micro}$[b] $cm^3\ g^{-1}$ | $V_{meso}$[c] $cm^3\ g^{-1}$ | $V_{total}$[d] $cm^3\ g^{-1}$ |
|---|---|---|---|---|
| ZTC | 4030 | 1.69 | 0.09 | 1.78 |
| MSC30 | 2690 | 1.12 | 0.61 | 1.73 |
| A20 | 1650 | 0.64 | 0.27 | 0.91 |

[a] *BET surface area ($p/p_0 = 0.01–0.05$).*
[b] *Micropore volume calculated by the Dubinin–Radushkevich equation.*
[c] $V_{total}–V_{micro}$.
[d] *Total pore volume estimated from the adsorption of $N_2$ at $p/p_0 = 0.96$.*

double-layer capacitors, because mesopores usually lower the density of the porous materials, resulting in a lower energy density per unit volume.

## 10.4. MOLECULAR STRUCTURE OF ZTC

Since we first succeeded in the synthesis of ZTC in 2000 [8], many researchers have been working on the development of several types of ZTCs, using several types of zeolite templates and carbon sources. However, its molecular structure had been completely unclear for a long period, because lattice fringes of graphene sheets can never be observed even with high-resolution TEM (Fig. 10.4b). Then, we made a great effort on analyzing ZTC structure with a variety of methods, and finally unveiled that its framework is comprised of cross-linked buckybowl-like nanographenes, which is a completely new nanocarbon form of $sp^2$ carbon network. In this section, the process of determining the molecular structure is presented.

### 10.4.1. Information Obtained from Various Kinds of Analysis

It has been known that ZTC is a negative replica of zeolite template from the results of SEM, TEM, and XRD, as shown in Figs 10.3–10.5. TEM and XRD results clearly indicate that ZTC has an ordered network structure which is replicated along with the pore network structure of the zeolite, and the ordered network has the same symmetry structure ($F\,d\,\overline{3}\,m$) as C–C network in a diamond crystal (Fig. 10.1c). As was described in the Section 10.3.2, the XRD pattern of ZTC does not show carbon (002) nor (10) peaks, indicating that this carbon contains neither graphene-stacking structure nor large and flat graphene plane. This is reasonable considering the size of the zeolite pores. Figure 10.8 compares the sizes of the zeolite pore and several molecules, benzene, coronene, and fullerene ($C_{60}$). The spherical zeolite pore (supercage) is only 1.3 nm,

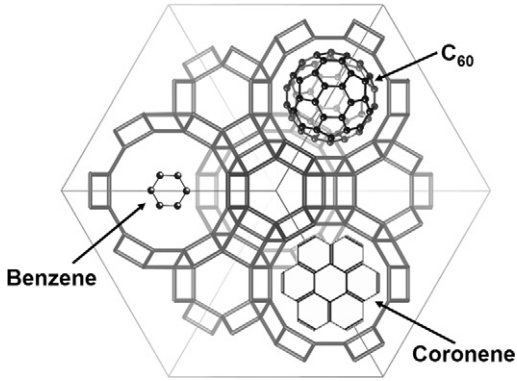


**FIGURE 10.8** Comparison of a supercage of zeolite Y and several molecules. A Si–O–Si bond is expressed by a line. Dodecagons surrounding benzene, coronene, or $C_{60}$ correspond to the supercage. This image is from the (111) direction of zeolite Y.

and the size barely allows coronene or $C_{60}$ to be included. Accordingly, a large graphite crystal never forms in such a small nanospace due to the structure hindrance. The ZTC framework must be comprised of very small carbonaceous fragments whose sizes are less than 1.3 nm.

ZTC has several characteristics which are typically seen in $sp^2$-carbon materials, such as black color, hydrophobicity, and electrical conductivity. The results of $^{13}C$ NMR [27] and electron energy-loss near-edge fine structure spectra [23] indeed show the presence of $sp^2$ carbons in ZTC, and $sp^3$ carbons are not detected. ZTC is therefore mainly comprised of $sp^2$ carbons.

In order to obtain further information on the $sp^2$-carbon framework, we measured Raman spectrum of ZTC and compared it with those of the reference carbons (Fig. 10.9). ZTC exhibits some typical Raman features for carbon

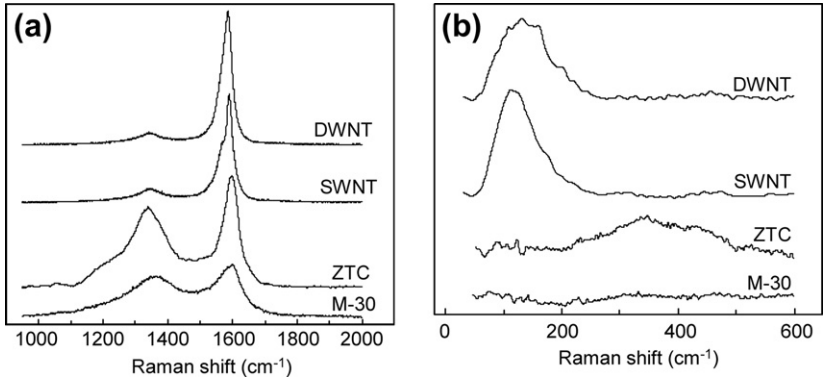


**FIGURE 10.9** Raman spectra of ZTC and some reference carbons [double- and single-walled carbon nanotubes (DWCNT and SWCNT) and activated carbon M-30] recorded with 488 nm laser line. (a) High-frequency Raman spectra and (b) low-frequency Raman spectra. *(Reprinted with permission from Ref [23]. Copyright 2009 Elsevier)*

materials: the tangential G band around 1598 $cm^{-1}$ and the defect-induced D band around 1345 $cm^{-1}$. Such intense G band directly indicates the significant presence of graphene sheets in ZTC, and D band indicates that the graphene has defects such as edge site. Additionally, the XRD pattern and the TEM observation did not show any evidence for sheet stacking of the nanographenes (Figs 10.4 and 10.5). These findings indicate that this carbon is made up by the assembly of single nanographene sheets, but not by the assembly of stacked graphene sheets, as is common for carbon materials. In addition to the intense G and D bands, we observed a broad Raman feature below 500 $cm^{-1}$, i.e. in a frequency range similar to that commonly found for the radial breathing mode (RBM) vibrations of SWCNTs or DWCNTs [28,29]. Figure 10.9b shows the low-frequency Raman spectrum of ZTC, together with those of some reference carbon materials, i.e. SWCNTs, DWCNTs and activated carbon M-30 [23]. We see from Fig 10.9b that ZTC has a broad Raman feature between 230 and 480 $cm^{-1}$. In marked contrast, the M-30 sample does not have any features in this frequency range. Such Raman features as observed for ZTC have also been reported for other carbons that consist of, or at least contain, curved graphitic sheets of a very small diameter of curvature (below 2–3 nm), including some types of bent graphitic layers [30,31], carbon onions [32]. The band at 230–480 $cm^{-1}$ observed in the Raman spectrum of ZTC can therefore also be considered as an indication of the presence of curved graphene sheets with a very small diameter of curvature in this sample. The presence of such curved graphene sheets in ZTC is reasonable, because the sheets must be forced to accommodate themselves into the more or less spherical cavities (~1.3 nm in diameter) of the zeolite Y supercages and the ~0.74 nm wide necks interconnecting adjacent cavities.

### 10.4.2. Construction of Possible Molecular Model

Based on the experimental evidences described in the precious section, we attempted to construct a reasonable molecular model for ZTC that could fit into the three-dimensionally ordered pores of zeolite Y [23]. This model must be consistent with the structural information obtained by the different characterization techniques (Raman, XRD, TEM, $^{13}C$ NMR, and electron energy-loss near-edge fine structure spectra). In addition, we imposed the condition that the model structure must be energetically stable upon the geometry optimization calculation using the semi-empirical Hamiltonian PM5 in MOPAC. To adapt a graphene sheet to the zigzagged channels of the zeolite, the sheet has to be artificially curved, thereby consisting of not only hexagons but also pentagons and/or heptagons. There are very few possibilities to arrange these polygons in such strictly regulated nanospace. Moreover, the graphene sheet should display a tetrahedral network structure as shown in Fig. 10.1c. One possibility would be a negatively curved graphene network that is known as Schwarzite [33,34]. Figure 10.10(a and b) shows two of such possible carbon models where the

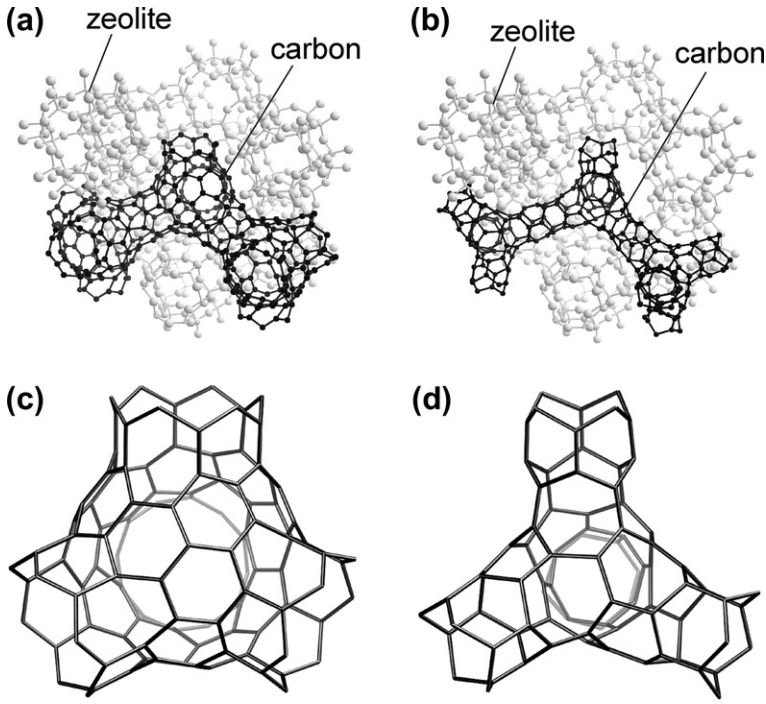


**FIGURE 10.10** Two hypothetical molecular structures of ZTC. The images (a) and (b) show the two ZTC models fitted into the framework of zeolite Y. (a) and (b) are comprised of building units (c) $C_{88}$ and (d) $C_{68}$, respectively, both of which have twelve heptagons. Note that one supercage of zeolite Y contains one building unit for both models. *(Reprinted with permission from Ref [23]. Copyright 2009 Elsevier)*

carbon atoms (black spheres) are interlinked with each other by $sp^2$-bonds to form a single and extremely curved graphene sheet with the three-dimensionally regular ordering. Each model is made up of building units, each of which fits into one supercage of zeolite Y. The units of models shown in Fig. 10.10a and b contain 88 and 68 carbon atoms (Fig. 10.10c and d), which respectively correspond to 0.67 and 0.52 g $g^{-1}$ of zeolite at the stage of the zeolite/carbon composites. A similar molecular model was also proposed by Roussel et al. with a statistical mechanics approach [35]. However, also these models have much larger amount of carbon against zeolite template compared to the amount experimentally obtained (0.29 g $g^{-1}$ of zeolite). If 50 carbon atoms were removed from the building unit of the model shown in Fig. 10.10a, its carbon content would become similar to the actual value. In the case of the model shown in Fig. 10.10b, 30 atoms must be eliminated. The removal of so many carbon atoms from each unit, however, inevitably leads to the collapse of the ordered structures of both models. Carbon frameworks composed of tubular graphenes are therefore different from the actual structure.

We then made every effort to construct other possible models, but always failed because the actual number of carbon atoms in zeolite is too small to construct a robust model. As mentioned before, in Fig. 10.10a and b, each building unit is tetrahedrally connected to four other units as shown in Fig 10.1c. However, we realized that, even if each building unit was not connected to all four other ones, but only to three others (Fig. 10.11a), the ordered structure could still be kept robust enough. Using this unsaturated structure, we again tried to construct an idealized molecular model for ZTC. Since the building unit shown in Fig. 10.11a (a black ball with three sticks) has a threefold axis, an idealized molecular model as the building unit should also have a threefold rotational symmetry. We finally found that the carbon model

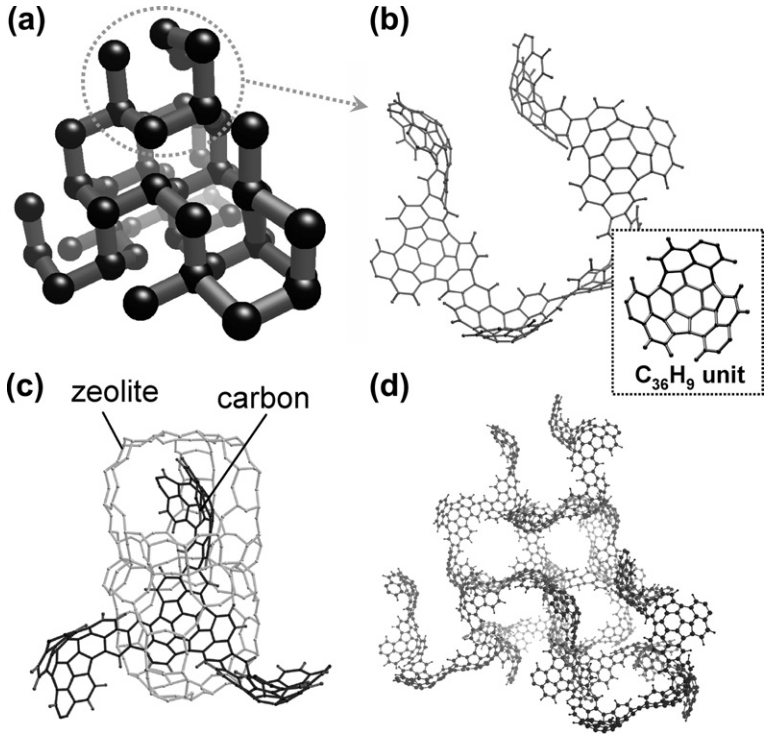


**FIGURE 10.11** Idealized molecular model containing only carbon and hydrogen atoms. (a) A ball and stick model for the structure of the ZTC framework. Black sphere and gray stick correspond to a basic buckybowl unit and the connection between two units, respectively. (b) An idealized molecular model constructed with six buckybowl units of $C_{36}H_9$ (inset). All the graphene edges are passivated with hydrogen atoms. The structure in (b) corresponds to the part indicated by a dotted circle in the network structure in (a). (c) The molecular model constructed with four buckybowl units with zeolite framework. (d) A large-sized molecular model that is constructed with the buckybowl units following the regularity of the zeolite Y template. The model (d) has the same network structure as the model (a). *(Reprinted with permission from Ref [23]. Copyright 2009 Elsevier)*

proposed in Fig. 10.11b met all the requirements. In this model, a basic building unit corresponding to a black sphere, shown in the inset of Fig. 10.11b, is a small curved graphene ($C_{36}H_9$, containing 3 pentagons), which is interlinked with three other units as indicated by the ordered framework structure in Fig. 10.11a. Note that the unit is quite similar to fullerene fragments, so-called buckybowls. The framework structure of this model looks unstable, but surprisingly the structure was energetically stable when the whole model shown in Fig. 10.11b was subjected to the geometry optimization calculation using the molecular orbital theory. Figure 10.11c shows the ZTC model embedded in the zeolite framework. It is clearly found that the present molecular model can fit the pore system of the zeolite. The amount of carbon in the model was calculated to be 0.28 g $g^{-1}$ of zeolite, which is very similar to the experimental value (0.29). In Fig. 10.11d, we present a large-sized idealized molecular model prepared from the buckybowls. Single and curved graphenes make up the three-dimensionally ordered network structure. We must emphasize that the steric hindrance imposed by the zeolite channels and the necessary number of carbon atoms are so strict that using $sp^2$-carbon atoms it was essentially impossible to make up any different network structures other than the present one.

ZTC actually contains a significant amount of oxygen as high as 8.9 wt% [23], which should be included in the idealized model of ZTC. Thus, we carried out the detailed analysis for oxygen functional groups. From the joint analysis using temperature programmed desorption (TPD) and FT-IR, we determined the quantities of oxygen functional groups, and constructed a modified molecular model in which the edge sites of the buckybowl units are occupied by appropriate types and amounts of functional groups, as shown in Fig. 10.12 [23]. Note that the whole structure (with the functional groups) shown in Fig. 10.12 was found to be energetically stable by the geometry optimization calculation using the molecular orbital theory.

In order to confirm the reliability of the proposed molecular model (Fig. 10.12), we compared numerical data of the model with these obtained by experiments, as summarized in Table 10.2 [23]. All of the values obtained from the model and experiments agree with each other very well.

Thus, we have proposed a possible molecular structure of ZTC, which possesses all the characteristics deduced from the experimental analyses of this material. This ordered microporous carbon is comprised of the assembly of single, nonstacked nanometer-sized graphene fragments, these nanographenes being curved like buckybowls due to the steric hindrance of the zeolite nanochannels in which they are formed. This three-dimensionally ordered and highly porous buckybowl-based structure is unique among any $sp^2$-bonded carbon materials produced so far. Although the actual carbon material will differ a little from this ideal model, the former can be thought of as a distorted version of the latter (*via* addition/removal of carbon atoms from, or twisting of, the buckybowls, etc), which still retains main features of the idealized model. The present model can therefore be considered as a reasonable starting point for

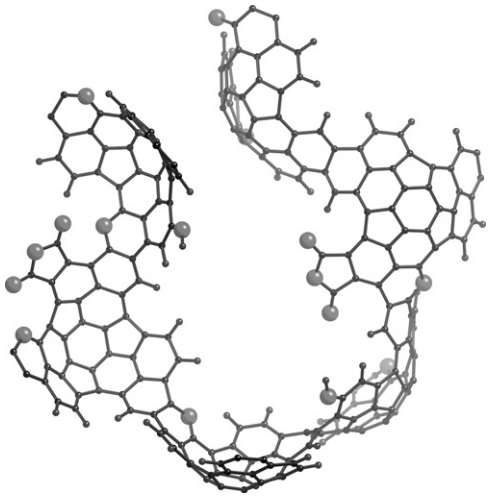

**FIGURE 10.12** An idealized model of ZTC containing functional groups (7 esters, 2 phenolic hydroxyl groups, 2 acid anhydride and 1 carboxyl group), adjusted to reflect the results of FT-IR and TPD. Large spheres indicate O atoms. *(Reprinted with permission from Ref [23]. Copyright 2009 Elsevier)*

future refinements of the structure of this quite novel carbon material and also for the theoretical modeling and understanding of ever-found and to-be-found interesting properties of ZTC, such as its high $H_2$ adsorption capacity and high performance as an electrode material for electric double-layer capacitors, as explained in the later sections.

### 10.4.3. Origin of the Extremely Large Surface Area of ZTC

ZTC shows an extremely high BET surface area of 4030 $m^2\ g^{-1}$ (Table 10.1). It should be noted that this value is estimated by the BET method, which usually

**TABLE 10.2** Comparison of Numerical Data Obtained From Experiments and Molecular Model Shown in Figure 10.12

| | Experiment [23] | Model |
|---|---|---|
| Carbon amount in carbon/zeolite composite (wt%) | 22 | 23 |
| Graphene curvature (nm) | 0.5–1.1 | 0.9–1.3 |
| Pore diameter (nm) | 1.0–1.5 | 1.0–1.7 |
| Micropore volume ($cm^3\ g^{-1}$) | 1.8 | 1.71 |
| Surface area ($m^2\ g^{-1}$)[a] | 3730 | 3432 |

[a]*Surface area calculated by the SPE method [36].*

causes an overestimation especially in the calculation for microporous carbons [36]. For ZTC, its real surface area can be actually estimated to be 3432 $m^2\ g^{-1}$, from its molecular structure shown in Fig. 10.12 [23]. Thus, the geometrical surface area of ZTC is over the theoretical surface area of both sides of a single graphene, 2627 $m^2\ g^{-1}$. The reason for this extraordinary high surface area is the contribution of the edge planes. Figure 10.13 illustrates geometrical surface areas of graphene (Fig. 10.13a), polycyclic aromatic compounds (Fig. 10.13b and c), and benzene (Fig. 10.13d). It is well known that the theoretical surface area of both sides of an infinity large graphene is 2627 $m^2\ g^{-1}$ (Fig. 10.13a), where the contribution of edge planes (Fig. 10.13b) is not considered. However, the contribution of the edge plane becomes significant when the size of graphene is less than several nanometers, and therefore, the geometrical surface area could be larger than 2627 $m^2\ g^{-1}$ in nanographenes (Fig. 10.13b–d). Accordingly, ZTC which is composed of the nanographene network (Fig. 10.12) has the extraordinary high surface area due to a large amount of edge planes.

Recently, "graphene" or "graphene-based materials" have attracted significant attention and many researchers are trying to use them for various kinds of applications including for adsorbents, considering its large theoretical surface area of 2627 $m^2\ g^{-1}$. It should, however, be noted that most of graphene surface is usually hidden and not fully available for adsorption. For example, the actual BET surface area of the reported "graphene-based material" was as low as 705 $m^2\ g^{-1}$ [37], indicating that more than 2/3 surface of the graphenes is not exposed to the outside. This is due to the aggregation of graphenes by strong van der Waals interaction. In order to expose the entire surface, graphene has to be formed into a self-standing three-dimensional network, like a pillared graphene which has been proposed by Froudakis et al. in their theoretical

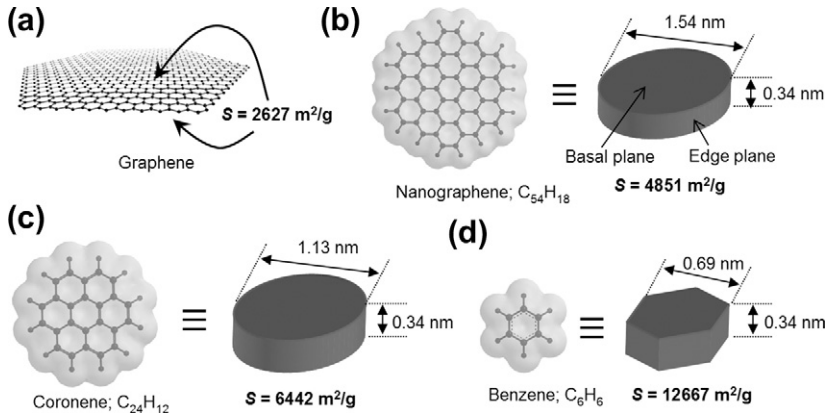


**FIGURE 10.13** Molecular models and the corresponding geometrical surface areas of (a) graphene, (b) nanographene ($C_{54}H_{18}$), (c) coronene, and (d) benzene.

work [38]. In this sense, ZTC does have an ideal three-dimensional structure (Fig. 10.11d) where the entire surface of the nanographene components is fully exposed to outside and can contribute to adsorption.

### 10.4.4. Comparison with Ordered Mesoporous Carbons

The first report for the synthesis of ZTC was actually done by our group in 1997 [2]. In this report, we used zeolite as a template and synthesized microporous carbons basically according to the same synthesis scheme as Fig. 10.1. Unfortunately, at that time, we did not confirm the replication of zeolite-ordered structure by the obtained carbons. We have then confirmed that ZTC has an ordered structure derived from zeolite template in 2000 [8].

In 1999, two Korean groups separately developed the method to obtain ordered mesoporous carbons (OMCs), according to the similar synthesis scheme to Fig. 10.1 but using mesoporous silica as hard templates (Fig. 10.14) [39,40]. Mesopores silica has much larger pores (>2 nm) than zeolite (<1.3 nm), and therefore, carbon introduction can be more easily achieved than the case of zeolite. From its easy synthesis procedure, OMC attracted a great deal of attention, and rapidly spread worldwide.

Because of their similar synthesis procedure, sometimes ZTC and OMC are not clearly distinguished from each other, rather they are regarded as similar materials having uniform nanopores. However, they are completely different carbon materials based on their molecular-level structures, as zeolites are different from mesoporous silicas. Figure 10.15 illustrates molecular-level structures of OMC [39–41] and ZTC together with their specific features. OMC has a uniform structure derived from the mesoporous silica template, but the framework itself is a disordered carbon which contains graphene-stacking structure and random micropores, like activated carbons. Thus, the microscopic structure of OMC is intrinsically different from that of ZTC, i.e. single nanographene network. The different framework structures make their pore structure also very much different. OMC has a uniform mesopores and also has random micropores inside the framework. Accordingly, OMC has a bimodal pore-size distribution both in micro- and mesopore regions. On the other hand,

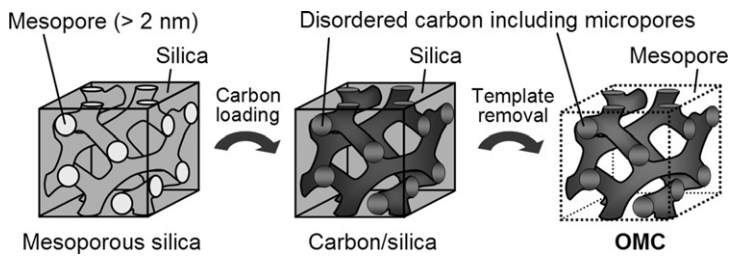


**FIGURE 10.14** Synthesis scheme of the ordered mesoporous carbon (OMC).

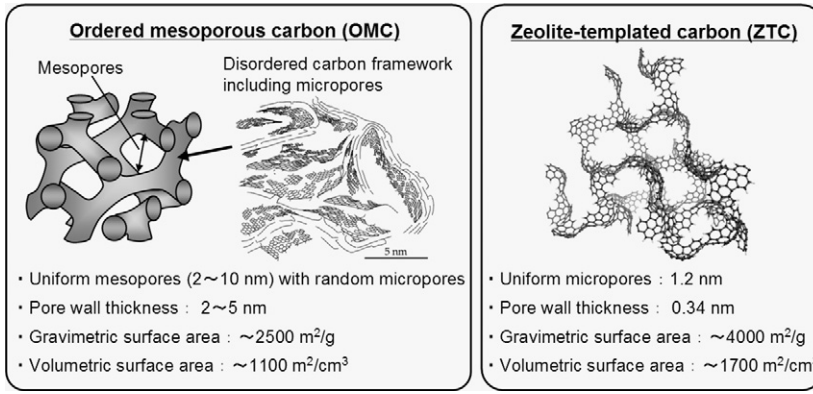


**FIGURE 10.15** Illustrations and specific features of ordered mesoporous carbon (OMC) and zeolite-templated carbon (ZTC).

ZTC is comprised of single nanographenes forming unimodal micropores with the size of 1.2 nm, and there are no other extrapores, such as ultramicropores, mesopores, and macropores. Due to the presence of micropores, OMC has a high gravimetric surface area of 2500 $m^2\ g^{-1}$, whereas its volumetric surface area is no more than 1100 $m^2\ cm^{-3}$, because the presence of large mesopores makes the density of carbon significantly low. Note that the volumetric surface area is calculated by (gravimetric surface area) × (density of carbon particle). On the other hand, ZTC has not only high gravimetric surface area (ca. 4000 $m^2\ g^{-1}$) but also very high volumetric surface area (1700 $m^2\ cm^{-3}$), due to the absence of larger pores. The volumetric surface area is very important to achieve high energy density per unit volume.

## 10.5. APPLICATION FOR HYDROGEN STORAGE

A fuel cell vehicle is a next-generation automobile that uses an energy source other than crude oil derivatives. However, there are several problems that should be solved before practical use. One of them is how to store hydrogen; that is, the development of a safe and efficient hydrogen-storage system is required [42]. There are several methods to store hydrogen: cryogenic liquid, compressed gas, metal hydrides, and adsorption. Each of them has advantages and disadvantages. Among these methods, adsorption of hydrogen in porous solids, especially carbon materials, is an attractive choice. They enjoy a long lifecycle, high durability, and hydrogen release at low temperature but lack sufficient storage capacity at room temperature. On the basis of physisorption, large surface area [43,44], large micropore volume [45–47], and a suitable pore size [45,46,48] are highly desirable for carbon materials to store enough hydrogen at room temperature. Highly microporous carbons are therefore the

most promising, rather than carbon nanotubes or carbon nanofibers. In the conventional chemical activation, larger surface area can be obtained under severe activation conditions, but at the same time, such activation significantly increases the amount of unnecessary mesopores. It is thus very difficult to achieve very high surface area and appropriate pore size simultaneously by conventional activation methods.

ZTC can overcome this problem. Several groups have reported the hydrogen-storage performance of several types of ZTCs at –196 °C [11,20,35,49,50]. It is noteworthy that Mokaya and co-workers [11] showed that ZTC exhibits the highest hydrogen uptake capacity among porous materials, including porous carbons, carbon nanotubes, zeolites, and metal–organic frameworks. In addition, Lachawiec and Yang [51] have reported noticeable large hydrogen uptake on ZTC at room temperature (up to 10 MPa). Our group has reported that ZTC exhibits a superior storage capacity especially at ultrahigh pressure range at room temperature [52]. Figure 10.16 shows hydrogen adsorption isotherms of ZTC and a high surface area activated carbon (MSC30, see Table 10.1) up to 34 MPa. In MSC30, its isotherm apparently levels off above 20 MPa, and it almost reaches the ceiling at 30 MPa. However, ZTC does not level off up to 34 MPa. Cazorla-Amorós and co-workers [45] have measured high-pressure hydrogen isotherms of various kinds of activated carbons at room temperature up to 70 MPa. They reported that most of the activated carbons reached a plateau above 20 MPa, but some showed almost no leveling off even at 70 MPa. They explained that there is an optimal pore size that can enhance the adsorption. The optimal pore size changes with the storage pressure. Kowalczyk et al. [48] have theoretically predicted that, in the case of carbon slit pores at 30 °C, 0.65 nm is optimum below 30 MPa and the optimal pore size is increased to 2.13 nm at 50 MPa. Thanks to the zeolite template, ZTC contains only such suitable-sized micropores (about 1.2 nm) for the enhancement effect. ZTC thus can exhibit one of the highest storage amounts (2.2 wt % at 30 °C and 34 MPa) among any pure carbon materials.

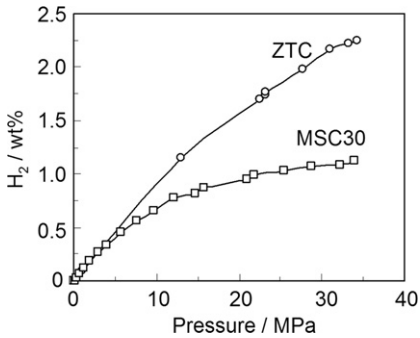


**FIGURE 10.16** Hydrogen adsorption isotherms of ZTC and MSC30 up to 34 MPa, measured at 30 °C. *(Reprinted with permission from Ref [52]. Copyright 2009 American Chemical Society)*

## 10.6. APPLICATION FOR ELECTRICAL DOUBLE-LAYER CAPACITORS

Electric double-layer capacitor (EDLC) is one of the key energy-storage devices for the development of clean energy technology including next-generation electric vehicles [53]. EDLC is charged in principle through the physisorption of electrolyte ions onto nanopore surfaces of a carbon electrode. Before the ions are adsorbed, they need to migrate from a bulk solution to the electrode surface through the narrow nanopores. Thus, the reduction of the ion-transfer resistance in the nanopores is one of the key issues to realize a high-power density EDLC [54–56]. Thus far, great efforts have been made to produce nanostructured electrode materials that possess efficient paths for ion diffusion. The successful examples are single-walled carbon nanotubes (SWCNTs) [57–59], templated mesoporous carbons (TMCs) [54,55], and hierarchical porous carbons (HPCs) [60,61]. These high-rate materials are characterized with large diffusion paths, the sizes of which are much larger than the size of solvated ions (~0.5 to 1.4 nm) [62], allowing the ions to move very rapidly during the charge/discharge processes. Consequently, these materials can retain their capacitance even at an ultrahigh current, i.e. exhibiting a high-rate performance, which is essential to construct a high-power density EDLC. However, paths that are too large make the electrode density significantly low and thus seriously decrease the volumetric capacitance, eventually resulting in the low volumetric energy density of the final EDLC device [60]. To avoid this problem, the size of the diffusion path should be as small as possible, but the fast ion transport has to be retained.

We have demonstrated that it is possible to meet the two seemingly contradictory requirements with ZTC, which can be clearly distinguished from TMCs with narrow pore-size distributions in the mesopore range (>2 nm) and therefore with the low volumetric capacitance [56,63]. Table 10.3 summarizes gravimetric ($S_g$) and volumetric ($S_v$) surface areas for several high-rate materials reported so far. In principle, $S_g$ and $S_v$ have directly to do with the gravimetric and the volumetric capacities, respectively. It is clear that ZTC has a great potential for higher capacity, especially for the volumetric one, compared with the others.

Figure 10.17 shows the change of the volumetric capacitances with the current density in 1 M $Et_4NBF_4$/propylene carbonate (PC) electrolyte solution at 25 °C. Two types of ZTCs are compared with activated carbons. ZTC-S has a higher surface area of 3690 $m^2\ g^{-1}$, while ZTC-L has a lower surface area of 2910 $m^2\ g^{-1}$ but has a better electric conductivity. Note that a larger current density corresponds to a faster discharge rate. In the low-current region below 2 $A\ g^{-1}$, all the ZTCs and the activated carbons show larger volumetric capacities than those of the high-rate materials (SWCNT [58] shows 22 $F\ cm^{-3}$ at 10 $A\ g^{-1}$, and HPC [60] shows 39 $F\ cm^{-3}$ at 4 $A\ g^{-1}$) due to their high volumetric surface areas. However, A20, a microporous activated carbon (Fig. 10.7b), cannot retain the capacitance, which decreases rapidly with increasing the current. MSC30, a carbon with some mesopores (Fig. 10.7b), retains 40% of its initial capacitance even at an ultrahigh current density of

**TABLE 10.3** Gravimetric ($S_g$) and Volumetric ($S_v$) Surface Areas of the High-Rate Materials Reported So Far [63]

| Carbon | $S_g$ [$m^2$ $g^{-1}$] | $S_v$ [$m^2$ $cm^{-3}$][a] | Reference |
|---|---|---|---|
| SWCNT | ~1000 | ~600 | [58] |
| TMC | ~1700 | ~900 | [55] |
| HPC | ~2060 | <510[b] | [60,61] |
| ZTC | ~3040 | ~1460 | [56] |

[a] *$S_v = S_g \rho$, where $\rho$ is the particle density of carbon. $\rho$ was calculated by $\rho = \{V_{total} + 1/\rho_{carbon}\}^{-1}$, where $V_{total}$ is the total pore volume estimated from $N_2$ isotherm (77 K) and $\rho_{carbon}$ is the true density of carbon (2 g $cm^{-3}$).*

[b] *$\rho$ of HPC was calculated without considering the total macropore volume because of a lack of the data in the reference. Therefore $S_v$ of HPC could actually be much less than 510 $m^2$ $cm^{-3}$.*

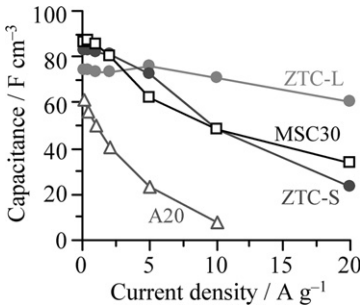


**FIGURE 10.17** Volumetric capacitance ($C_v$) versus current density for two types of ZTCs (ZTC-S and ZTC-L) and activated carbons (MSC30 and A20). $C_v$ was calculated by $C_v = C_s F$, where $C_s$ is a gravimetric capacitance obtained by galvanostatic charge–discharge cycling, and $F$ is the particle density (see Table 10.3). *(Reprinted with permission from Ref [63]. Copyright 2011 American Chemical Society)*

20 A $g^{-1}$. These results are in accord with the general tendency in the references [55,56,60,61], i.e. larger nanopores can accelerate ion-transfer, and as a result, a better-rate performance is achieved. On the other hand, ZTCs can well retain the capacitance in the ultrahigh current region, although their nanopore sizes (~1.2 nm) are less than those of MSC30. This high-rate performance can be ascribed to their 3D and mutually connected nanopore arrangement.

## 10.7. GENERAL CONCLUSION AND PERSPECTIVES

ZTC has a 3D ordered framework composed of buckybowl-like nanographenes, thereby making it extraordinary $sp^2$-based carbon material. In addition, ZTC has a huge adsorption capability together with a uniform micropore size (ca. 1.2 nm), and such characteristics make this material a very attractive adsorbent, especially for energy storage such as hydrogen storage and EDLC as described in this chapter. With its extremely unique structure and properties, ZTC can be a next-generation 3D graphene-based architecture which follows fullerene (0D), carbon nanotube (1D), and graphene (2D).

Since the discovery of ZTC [1,2,8], many different research groups have dealt with this very unique carbon material, and the works related to ZTC are now becoming to be a new research field. As described in the Section 10.2, various types of ZTCs with different structures have been synthesized so far. However, there is still great possibility for the synthesis of further new ZTCs. One possible method is the use of new zeolite templates which meet the requirements described in the Section 10.2.1, for producing new types of ZTCs with different framework regularities from the conventional ZTCs synthesized with FAU, BEA, and EMT. There are actually many possible candidates for a hard template, considering the numerous types of zeolite crystals (>190). Even by using the same zeolite template, various different types of ZTCs are possibly produced by changing the carbon source, carbon introduction amount into zeolite, and heat-treatment conditions. In addition, postsynthesis modification is expected to be further developed because ZTC has a large amount of edge sites which are fully exposed and highly reactive. ZTC-based composite materials are also of interest. There have been several reports for Pt-loaded ZTC with regard to its promising applications in fuel cells [10,64] or hydrogen storage [52,65]. Not only Pt but also other kinds of metals, metal oxides, and organic compounds could be combined with ZTC to form new composite materials with superior performances.

It should be emphasized that ZTC is attractive not only as high-performance sorbents and/or energy storage media but also as model porous materials for understanding the basic phenomena related to micropores, as we have demonstrated in the research on EDLC [56]. We believe that a family of ZTC materials will be further developed hereafter, which could open the door for new nanocarbon technology involving batteries, gas storage, catalysts, and any other fields.

## ACKNOWLEDGMENTS

This work was partially supported by KAKENHI (Grant-in-Aid for Scientific Research) on the Priority Area 'New Materials Science Using Regulated Nano Spaces-Strategy in Ubiquitous Elements' from the Ministry of Education, Culture, Sports, Science and Technology of Japan (T.K.) for the Sections 10.3 and 10.4; by NEDO (T.K.) for the Section 10.5; by Grant-in-Aid for Scientific Research on the Innovative Areas: "Fusion Materials" (Area no. 2206) from the Ministry of Education, Culture, Sports, Science and Technology (H.N.) for the Sections 10.3 and 10.4; and by Japan Society of the Promotion of Science, Grant-in-Aid for young scientists (A), 23685041 (H.N.) for the Sections 10.2 and 10.6.

## REFERENCES

[1] T. Kyotani, T. Nagai, A. Tomita, Preparation of New Carbon from Zeolite as Template. Extended Abstracts of Carbon '92, 1992. pp. 437–439.

[2] T. Kyotani, T. Nagai, S. Inoue, A. Tomita, Formation of new type of porous carbon by carbonization in zeolite nanochannels, Chem. Mater. 9 (1997) 609–615.

[3] P. Enzel, T. Bein, Poly(acrylonitrile) chains in zeolite channels – polymerization and pyrolysis, Chem. Mater. 4 (1992) 819–824.
[4] T. Cordero, P.A. Thrower, L.R. Radovic, On the oxidation resistance of carbon–carbon composites obtained by chemical vapor infiltration of different carbon cloths, Carbon 30 (1992) 365–374.
[5] J. Rodriguez-Mirasol, T. Cordero, L.R. Radovic, J.J. Rodriguez, Structural and textural properties of pyrolytic carbon formed within a microporous zeolite template, Chem. Mater. 10 (1998) 550–558.
[6] S.A. Johnson, E.S. Brigham, P.J. Ollivier, T.E. Mallouk, Effect of micropore topology on the structure and properties of zeolite polymer replicas, Chem. Mater. 9 (1997) 2448–2458.
[7] C.J. Meyers, S.D. Shah, S.C. Patel, R.M. Sneeringer, C.A. Bessel, N.R. Dollahon, R.A. Leising, E.S. Takeuchi, Templated synthesis of carbon materials from zeolites (Y, beta, and ZSM-5) and a montmorillonite clay (K10): physical and electrochemical characterization, J. Phys. Chem. B 105 (2001) 2143–2152.
[8] Z.X. Ma, T. Kyotani, A. Tomita, Preparation of a high surface area microporous carbon having the structural regularity of Y zeolite, Chem. Commun. (2000) 2365–2366.
[9] T. Kyotani, Z.X. Ma, A. Tomita, Template synthesis of novel porous carbons using various types of zeolites, Carbon 41 (2003) 1451–1459.
[10] F.B. Su, H.J. Zeng, Y.J. Yu, L. Lv, J.Y. Lee, X.S. Zhao, Template synthesis of microporous carbon for direct methanol fuel cell application, Carbon 43 (2005) 2368–2373.
[11] Z.X. Yang, Y.D. Xia, R. Mokaya, Enhanced hydrogen storage capacity of high surface area zeolite-like carbon materials, J. Am. Chem. Soc. 129 (2007) 1673–1679.
[12] F.O.M. Gaslain, J. Parmentier, V.P. Valtchev, J. Patarin, First zeolite carbon replica with a well resolved X-ray diffraction pattern, Chem. Commun. (2006) 991–993.
[13] K. Hernadi, A. Fonseca, J.B. Nagy, D. Bernaerts, A. Fudala, A.A. Lucas, Catalytic synthesis of carbon nanotubes using zeolite support, Zeolites 17 (1996) 416–423.
[14] K. Mukhopadhyay, A. Koshio, T. Sugai, N. Tanaka, H. Shinohara, Z. Konya, J.B. Nagy, Bulk production of quasi-aligned carbon nanotube bundles by the catalytic chemical vapour deposition (CCVD) method, Chem. Phys. Lett. 303 (1999) 117–124.
[15] A. Garsuch, O. Klepel, Synthesis of ordered carbon replicas by using Y-zeolite as template in a batch reactor, Carbon 43 (2005) 2330–2337.
[16] A. Garsuch, O. Klepel, R.R. Sattler, C. Berger, R. Glaser, J. Weitkamp, Synthesis of a carbon replica of zeolite Y with large crystallite size, Carbon 44 (2006) 593–596.
[17] F.B. Su, L. Lv, T.M. Hui, X.S. Zhao, Phenol adsorption on zeolite-templated carbons with different structural and surface properties, Carbon 43 (2005) 1156–1164.
[18] F.B. Su, X.S. Zhao, L. Lv, Z.C. Zhou, Synthesis and characterization of microporous carbons templated by ammonium-form zeolite Y, Carbon 42 (2004) 2821–2831.
[19] P.X. Hou, T. Yamazaki, H. Orikasa, T. Kyotani, An easy method for the synthesis of ordered microporous carbons by the template technique, Carbon 43 (2005) 2624–2627.
[20] Z.X. Yang, Y.D. Xia, X.Z. Sun, R. Mokaya, Preparation and hydrogen storage properties of zeolite-templated carbon materials nanocast via chemical vapor deposition: effect of the zeolite template and nitrogen doping, J. Phys. Chem. B 110 (2006) 18424–18431.
[21] K. Matsuoka, Y. Yamagishi, T. Yamazaki, N. Setoyama, A. Tomita, T. Kyotani, Extremely high microporosity and sharp pore size distribution of a large surface area carbon prepared in the nanochannels of zeolite Y, Carbon 43 (2005) 876–879.
[22] P.X. Hou, H. Orikasa, T. Yamazaki, K. Matsuoka, A. Tomita, N. Setoyama, Y. Fukushima, T. Kyotani, Synthesis of nitrogen-containing microporous carbon with a highly ordered

structure and effect of nitrogen doping on $H_2O$ adsorption, Chem. Mater. 17 (2005) 5187–5193.

[23] H. Nishihara, Q.H. Yang, P.X. Hou, M. Unno, S. Yamauchi, R. Saito, J.I. Paredes, A. Martinez-Alonso, J.M.D. Tascon, Y. Sato, M. Terauchi, T. Kyotani, A possible buckybowl-like structure of zeolite templated carbon, Carbon 47 (2009) 1220–1230.

[24] M. Kruk, M. Jaroniec, R. Ryoo, S.H. Joo, Characterization of ordered mesoporous carbons synthesized using MCM-48 silicas as templates, J. Phys. Chem. B 104 (2000) 7960–7968.

[25] J.S. Lee, S.H. Joo, R. Ryoo, Synthesis of mesoporous silicas of controlled pore wall thickness and their replication to ordered nanoporous carbons with various pore diameters, J. Am. Chem. Soc. 124 (2002) 1156–1157.

[26] C. Vix-Guterl, S. Saadallah, L. Vidal, M. Reda, J. Parmentier, J. Patarin, Template synthesis of a new type of ordered carbon structure from pitch, J. Mater. Chem. 13 (2003) 2535–2539.

[27] Z.X. Ma, T. Kyotani, Z. Liu, O. Terasaki, A. Tomita, Very high surface area microporous carbon with a three-dimensional nano-array structure: synthesis and its molecular structure, Chem. Mater. 13 (2001) 4413–4415.

[28] M.S. Dresselhaus, G. Dresselhaus, R. Saito, A. Jorio, Raman spectroscopy of carbon nanotubes, Phys. Rep. 409 (2005) 47–99.

[29] M.S. Dresselhaus, P.C. Eklund, Phonons in carbon nanotubes, Adv. Phys. 49 (2000) 705–814.

[30] Y. Gogotsi, J.A. Libera, N. Kalashnikov, M. Yoshimura, Graphite polyhedral crystals, Science 290 (2000) 317–320.

[31] J.J. Wang, M.Y. Zhu, R.A. Outlaw, X. Zhao, D.M. Manos, B.C. Holloway, V.P. Mammana, Free-standing subnanometer graphite sheets, Appl. Phys. Lett. 85 (2004) 1265–1267.

[32] D. Roy, M. Chhowalla, H. Wang, N. Sano, I. Alexandrou, T.W. Clyne, G.A.J. Amaratunga, Characterisation of carbon nano-onions using Raman spectroscopy, Chem. Phys. Lett. 373 (2003) 52–56.

[33] T. Lenosky, X. Gonze, M. Teter, V. Elser, Energetics of negatively curved graphitic carbon, Nature 355 (1992) 333–335.

[34] V. Rosato, M. Celino, G. Benedek, S. Gaito, Thermodynamic behavior of the carbon schwarzite fcc $(C_{36})_2$, Phys. Rev. B 60 (1999) 16928–16933.

[35] T. Roussel, A. Didion, R.J.M. Pellenq, R. Gadiou, C. Bichara, C. Vix-Guterl, Experimental and atomistic simulation study of the structural and adsorption properties of Faujasite zeolite-templated nanostructured carbon materials, J. Phys. Chem. C 111 (2007) 15863–15876.

[36] K. Kaneko, C. Ishii, M. Ruike, H. Kuwabara, Origin of superhigh surface-area and micro-crystalline graphitic structures of activated carbons, Carbon 30 (1992) 1075–1088.

[37] H.S. Zhou, S.M. Zhu, M. Hibino, I. Honma, M. Ichihara, Lithium storage in ordered mesoporous carbon (CMK-3) with high reversible specific energy capacity and good cycling performance, Adv. Mater. 15 (2003) 2107–2111.

[38] K.S. Xia, Q.M. Gao, C.D. Wu, S.Q. Song, M.L. Ruan, Activation, characterization and hydrogen storage properties of the mesoporous carbon CMK-3, Carbon 45 (2007) 1989–1996.

[39] R. Ryoo, S.H. Joo, S. Jun, Synthesis of highly ordered carbon molecular sieves via template-mediated structural transformation, J. Phys. Chem. B 103 (1999) 7743–7746.

[40] J. Lee, S. Yoon, T. Hyeon, S.M. Oh, K.B. Kim, Synthesis of a new mesoporous carbon and its application to electrochemical double-layer capacitors, Chem. Commun. (1999) 2177–2178.

[41] M. Sevilla, S. Alvarez, T.A. Centeno, A.B. Fuertes, F. Stoeckli, Performance of templated mesoporous carbons in supercapacitors, Electrochim. Acta 52 (2007) 3207–3215.

[42] L. Schlapbach, A. Zuttel, Hydrogen-storage materials for mobile applications, Nature 414 (2001) 353–358.

[43] M.K. Haas, J.M. Zielinski, G. Dantsin, C.G. Coe, G.P. Pez, A.C. Cooper, Tailoring single walled carbon nanotubes for hydrogen storage, J. Mater. Res. 20 (2005) 3214–3223.
[44] Y. Kojima, Y. Kawai, A. Koiwai, N. Suzuki, T. Haga, T. Hioki, K. Tange, Hydrogen adsorption and desorption by carbon materials, J. Alloys Compd. 421 (2006) 204–208.
[45] M.A. de la Casa-Lillo, F. Lamari-Darkrim, D. Cazorla-Amoros, A. Linares-Solano, Hydrogen storage in activated carbons and activated carbon fibers, J. Phys. Chem. B 106 (2002) 10930–10934.
[46] M. Jorda-Beneyto, F. Suarez-Garcia, D. Lozano-Castello, D. Cazorla-Amoros, A. Linares-Solano, Hydrogen storage on chemically activated carbons and carbon nanomaterials at high pressures, Carbon 45 (2007) 293–303.
[47] H. Takagi, H. Hatori, Y. Soneda, N. Yoshizawa, Y. Yamada, Adsorptive hydrogen storage in carbon and porous materials, Mater. Sci. Eng. B 108 (2004) 143–147.
[48] P. Kowalczyk, H. Tanaka, R. Holyst, K. Kaneko, T. Ohmori, J. Miyamoto, J. Phys. Chem. B 109 (2005) 17174–17183.
[49] L. Chen, R.K. Singh, P. Webley, Synthesis, characterization and hydrogen storage properties of microporous carbons templated by cation exchanged forms of zeolite Y with propylene and butylene as carbon precursors, Microporous Mesoporous Mater. 102 (2007) 159–170.
[50] A. Pacula, R. Mokaya, Synthesis and high hydrogen storage capacity of zeolite-like carbons nanocast using as-synthesized zeolite templates, J. Phys. Chem. C 112 (2008) 2764–2769.
[51] A.J. Lachawiec, R.T. Yang, Isotope tracer study of hydrogen spillover on carbon-based adsorbents for hydrogen storage, Langmuir 24 (2008) 6159–6165.
[52] H. Nishihara, P.X. Hou, L.X. Li, M. Ito, M. Uchiyama, T. Kaburagi, A. Ikura, J. Katamura, T. Kawarada, K. Mizuuchi, T. Kyotani, High-pressure hydrogen storage in zeolite-templated carbon, J. Phys. Chem. C 113 (2009) 3189–3196.
[53] R. Kotz, M. Carlen, Principles and applications of electrochemical capacitors, Electrochim. Acta 45 (2000) 2483–2498.
[54] K. Jurewicz, C. Vix-Guterl, E. Frackowiak, S. Saadallah, A. Reda, J. Parmentier, J. Patarin, F. Beguin, Capacitance properties of ordered porous carbon materials prepared by a templating procedure, J. Phys. Chem. Solids 65 (2004) 287–293.
[55] W. Xing, S.Z. Qiao, R.G. Ding, F. Li, G.Q. Lu, Z.F. Yan, H.M. Cheng, Superior electric double layer capacitors using ordered mesoporous carbons, Carbon 44 (2006) 216–224.
[56] H. Nishihara, H. Itoi, T. Kogure, P.X. Hou, H. Touhara, F. Okino, T. Kyotani, Investigation of the ion storage/transfer behavior in an electrical double-layer capacitor by using ordered microporous carbons as model materials, Chem. Eur. J. 15 (2009) 5355–5363.
[57] K.H. An, W.S. Kim, Y.S. Park, J.M. Moon, D.J. Bae, S.C. Lim, Y.S. Lee, Y.H. Lee, Electrochemical properties of high-power supercapacitors using single-walled carbon nanotube electrodes, Adv. Funct. Mater. 11 (2001) 387–392.
[58] D.N. Futaba, K. Hata, T. Yamada, T. Hiraoka, Y. Hayamizu, Y. Kakudate, O. Tanaike, H. Hatori, M. Yumura, S. Iijima, Shape-engineerable and highly densely packed single-walled carbon nanotubes and their application as super-capacitor electrodes, Nat. Mater. 5 (2006) 987–994.
[59] C.M. Niu, E.K. Sichel, R. Hoch, D. Moy, H. Tennent, High power electrochemical capacitors based on carbon nanotube electrodes, Appl. Phys. Lett. 70 (1997) 1480–1482.
[60] S.W. Woo, K. Dokko, H. Nakano, K. Kanamura, Preparation of three dimensionally ordered macroporous carbon with mesoporous walls for electric double-layer capacitors, J. Mater. Chem. 18 (2008) 1674–1680.

[61] H. Yamada, H. Nakamura, F. Nakahara, I. Moriguchi, T. Kudo, Electrochemical study of high electrochemical double layer capacitance of ordered porous carbons with both meso/macropores and micropores, J. Phys. Chem. C 111 (2007) 227–233.
[62] C.M. Yang, Y.J. Kim, M. Endo, H. Kanoh, M. Yudasaka, S. Iijima, K. Kaneko, Nanowindow-regulated specific capacitance of supercapacitor electrodes of single-wall carbon nanohorns, J. Am. Chem. Soc. 129 (2007) 20–21.
[63] H. Itoi, H. Nishihara, T. Kogure, T. Kyotani, Three-Dimensionally arrayed and mutually connected 1.2 nm-nanopores for high-performance electric double layer capacitor, J. Am. Chem. Soc. 133 (2011) 1165–1167.
[64] E.N. Coker, W.A. Steen, J.T. Miller, A.J. Kropf, J.E. Miller, The preparation and characterization of novel Pt/C electrocatalysts with controlled porosity and cluster size, J. Mater. Chem. 17 (2007) 3330–3340.
[65] Z. Wang, F.H. Yang, R.T. Yang, Enhanced hydrogen spillover on carbon surfaces modified by oxygen plasma. J. Phys. Chem. C, 114 (2010) 1601–1609.